Microfluidic production of single micrometer-sized hydrogel beads utilizing droplet dissolution in a polar solvent

Sari Sugaya, Masumi Yamada,[a] Ayaka Hori, and Minoru Seki
Department of Applied Chemistry and Biotechnology, Graduate School of Engineering, Chiba University, 1-33 Yayoi-cho, Inage-ku, Chiba 263-8522, Japan

(Received 30 August 2013; accepted 14 October 2013; published online 24 October 2013)

In this study, a microfluidic process is proposed for preparing monodisperse micrometer-sized hydrogel beads. This process utilizes non-equilibrium aqueous droplets formed in a polar organic solvent. The water-in-oil droplets of the hydrogel precursor rapidly shrunk owing to the dissolution of water molecules into the continuous phase. The shrunken and condensed droplets were then gelled, resulting in the formation of hydrogel microbeads with sizes significantly smaller than the initial droplet size. This study employed methyl acetate as the polar organic solvent, which can dissolve water at 8%. Two types of monodisperse hydrogel beads—Ca-alginate and chitosan—with sizes of 6–10 μm (coefficient of variation $< 6\%$) were successfully produced. In addition, we obtained hydrogel beads with non-spherical morphologies by controlling the degree of droplet shrinkage at the time of gelation and by adjusting the concentration of the gelation agent. Furthermore, the encapsulation and concentration of DNA molecules within the hydrogel beads were demonstrated. The process presented in this study has great potential to produce small and highly concentrated hydrogel beads that are difficult to obtain by using conventional microfluidic processes. © *2013 AIP Publishing LLC*.
[http://dx.doi.org/10.1063/1.4826936]

I. INTRODUCTION

Hydrogels are widely used in medicine and chemical and biological research for immobilizing and/or releasing bioactive compounds. Hydrogels are also employed as three-dimensional scaffolds for constructing living tissue models and as matrices for biomolecule separation and analysis.[1–3] Spherical beads are one of the most common forms of hydrogels, largely because of the ease of its preparation and manipulation. In general, the physicochemical characteristics and applications of hydrogel beads are closely associated with their size and monodispersity. Small beads with a high surface-to-volume ratio exhibit rapid diffusion-based molecular transport through their permeable matrices. Thus, the use of small and monodisperse hydrogel beads as bead-based stationary phases for separation columns and as cell-incorporating capsules for bioproduction and cell transplantation therapies is especially advantageous. In addition, the bead size is related to the uptake efficiency by cells and the release rate of drugs in hydrogel-based carriers for drug delivery systems (DDS).[4] Hence, the precise control of the size and the monodispersity of hydrogel beads is essential for conducting these applications.

To date, various techniques have been developed for the preparation of hydrogel microbeads. Monodisperse hydrogel beads were obtained using microfabrication and microfluidic technologies, in which droplets of a hydrogel precursor solution were generated by using micro-nozzles,[5–7] ink-jet devices,[8] and microfluidic channels.[9–15] The generated droplets were then gelled to form monodisperse spherical beads with diameters typically as large as 100 μm. In addition, non-spherical beads have been produced by employing photopolymerization-based techniques, such as

[a]Tel./Fax: +81-43-290-3398. E-mail: m-yamada@faculty.chiba-u.jp

stopped-flow lithography,[16–20] scanning-laser lithography,[21] micro-molding,[22] and continuous cross-linking,[23] or by utilizing multiphase microfluidics.[24] These non-spherical beads would be potentially useful as unit structures for fabricating large hydrogel-based constructs by 3D assembly and would also be advantageous for biological encapsulation due to their higher surface-to-volume ratios compared to the spherical beads. However, there exist very few techniques for preparing monodisperse hydrogel beads with sizes as small as single mammalian cells ($\sim$10 μm).[12,25–27] One of the reasons can be attributed to the difficulty in generating small droplets of viscous precursor solutions using microfabricated nozzles or microfluidic channels. In addition, controlling the morphologies of such small hydrogel beads so as to obtain non-spherical beads remains a challenge.

In this study, we present a simple but versatile microfluidic process based on the dissolution of the aqueous droplets of hydrogel precursor to produce monodisperse single micrometer-sized hydrogel beads. The procedure for producing micrometer-sized hydrogel beads is shown in Fig. 1. A polar organic solvent, which can dissolve a limited amount of water, and a diluted precursor solution are employed as the continuous and dispersed phases, respectively, and introduced into the microchannel. Water-in-oil (W/O) droplets are generated at the first confluence point, which rapidly shrink while flowing through the microchannel, resulting in the concentration of the hydrogel polymer molecules. This phenomena of the droplet dissolution, often referred to as solvent evaporation, has been utilized for producing synthetic polymer beads,[28,29] silica particles,[30,31] and polysaccharide beads,[32] and for assembling colloidal particles.[33–35] An aqueous solution of a gelation agent was introduced downstream into the microchannel, generating hydrogel beads significantly smaller than the initial droplets. We attempted to prepare two types of micrometer-sized hydrogel beads by using alginate and chitosan as the hydrogel material. In addition, we examined several factors that affect the size and the morphology of the beads such as the concentrations of the precursor and the gelation agent and the degree of water-molecule dissolution. Furthermore, we demonstrated the encapsulation of DNA molecules within the hydrogel beads.

II. EXPERIMENTAL SECTION

A. Microchannel fabrication and design

PDMS (Polydimethylsiloxane; Silpot-184 from Dow Corning Toray Co., Ltd., Japan) microchannels were prepared by using standard soft lithography and replica molding techniques

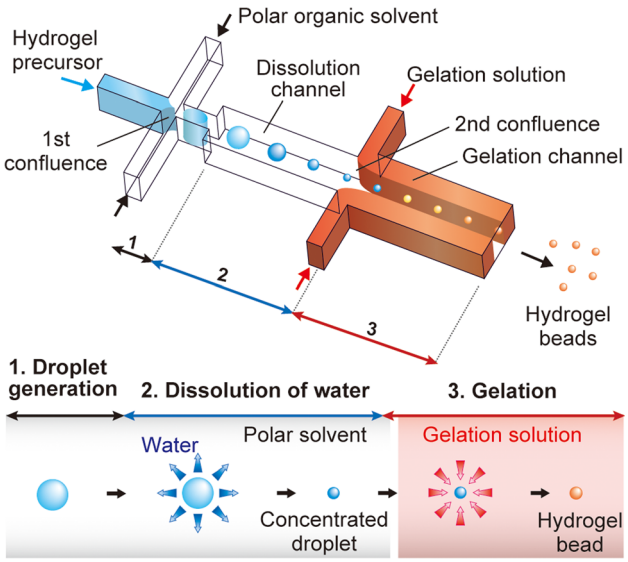

FIG. 1. Schematic illustrating the microfluidic process for producing single micrometer-sized hydrogel beads using non-equilibrium droplets. A polar organic solvent (methyl acetate) is employed as the continuous phase. Droplets of a diluted hydrogel precursor solution are formed, which shrink because of the dissolution of water into the continuous phase. The gelation solution is introduced at the second confluence point to produce hydrogel beads significantly smaller than the initial droplets.

as described elsewhere.[36] A PDMS replica was bonded to a flat PDMS plate via O_2 plasma treatment to form the microchannel structure. To ensure the recovery of the hydrophobicity of PDMS after the bonding process, the bonded PDMS microdevice was heated at 150 °C for at least 3 h before use. The microchannel design is shown in Fig. 2(a). There are 4 inlets: Inlet 1 for the organic solvent, Inlet 2 for the precursor solution, and Inlets 3 and 3′ for the gelation solution. The length of the water dissolution channel was either 22 or 70 mm, whereas that of the gelation channel was 75 mm. The width of the microchannel at the first confluence point was 50 μm, whereas that of the dissolution and the gelation channels was 200 μm. The microchannel depth across the entire device was 55 μm.

B. Production of hydrogel microbeads

In this study, methyl acetate was primary used as the polar organic solvent, unless otherwise noted. Water has a solubility of 8% in methyl acetate at room temperature. For producing alginate hydrogel beads, sodium alginate (NaA; Kimica IL-6, Kimica Corp., Japan) was

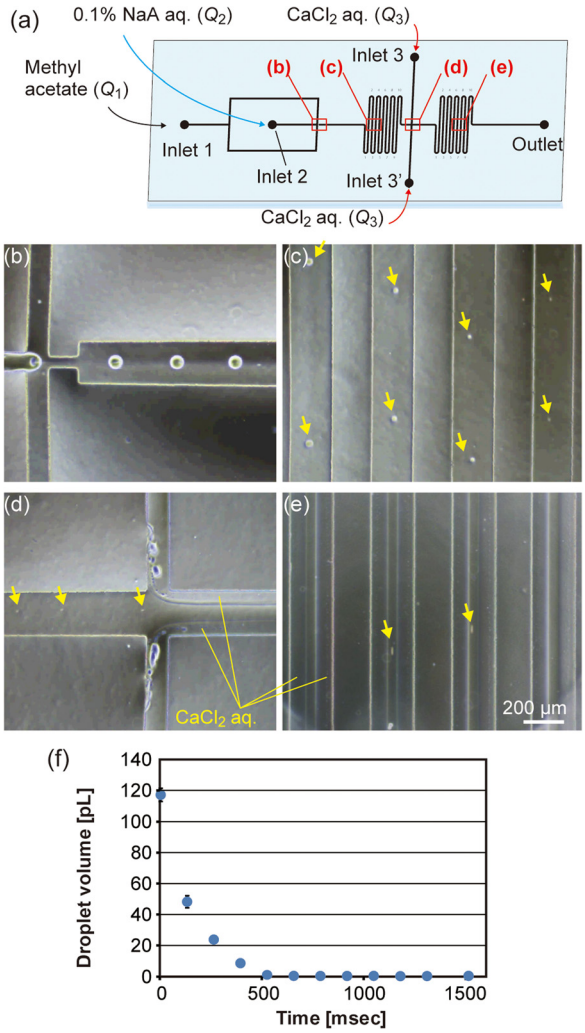

FIG. 2. Droplet formation and dissolution in the microchannel. (a) Schematic image showing the microfluidic device. (b)-(e) Micrographs showing the droplets of sodium alginate (NaA) solution, (b) at the first confluence, (c) in the dissolution channel, (d) at the second confluence, and (e) in the gelation channel. Methyl acetate, 0.1% sodium alginate (NaA) solution, and 1M $CaCl_2$ solution were used as the continuous phase, dispersed phase, and the gelation solution, respectively. In (c)–(e), small arrows indicate the droplets. (f) The change in the volume of the droplets flowing through the gelation channel over time. Each data show the mean ± SD value.

dissolved in distilled water. Methyl acetate, an aqueous solution of NaA (0.025%–0.15%), and an aqueous solution of 1M $CaCl_2$ were introduced into the microchannel by using syringe pumps (KDS200, KD Scientific, MA, USA) with flow rates of Q_1, Q_2, and Q_3 ($=Q'_3$), respectively. The formation of the droplets and the beads was observed using an inverted microscope (IX71, Olympus, Japan). The generated beads were continuously and directly collected from the microchannel into a glass vial through Teflon tubing. Collected beads were washed twice with 0.1M $CaCl_2$ solution to remove the remaining organic solvent. The size of the droplets and the beads was measured using an image processing software by analyzing at least 100 beads for each condition. For characterizing non-spherical beads, the longest axis (width or length) of the beads was determined from the captured micrographs.

In the experiment for producing chitosan hydrogel beads, 0.025% or 0.05% chitosan (deacetylation degree higher than 80%, viscosity of an aqueous solution of 1% (w/v) chitosan at 20 °C was measured to be 72.4 mPa·s, Wako Pure Chemical Ind. Ltd., Japan) in 0.1M acetic acid was used as the precursor solution, and 1 mM NaOH aq. was used as the gelation solution. The formed chitosan hydrogel beads were washed twice with distilled water, and the bead sizes were measured. In addition, the chitosan beads were fluorescently labeled; the obtained beads were dipped in 50 mM borate buffer (pH = 8.5) with 0.1 mg/ml N-hydroxysuccinimide (NHS)-conjugated fluorescein (Thermo Scientific, MA, USA) for 30 min and then washed several times with the borate buffer.

To prepare DNA-encapsulating hydrogel beads, λDNA (Takara Bio Inc., Japan) was dissolved in an aqueous solution of 0.1% NaA at a concentration of 50, 100, or 200 ng/μl. The prepared beads were then suspended in 0.1M $CaCl_2$ aq. supplemented with 0.01% SYBR Green I solution (10 000×, Biowhittaker Molecular Applications, ME, USA).

III. RESULTS AND DISCUSSION

A. Droplet formation and dissolution

First, we observed the formation and dissolution of the droplet using the microfluidic device with the dissolution channel-length of 70 mm. Figure 2 shows the formation of non-equilibrium droplets in the microchannel. Aqueous droplets of the hydrogel precursor (0.1% NaA aq.) were generated in the continuous phase at the first confluence point at a production rate of ∼100 droplets/s when Q_1 and Q_2 were 30 and 0.9 μl/min, respectively. The initial volume ± SD of the generated droplets was 175 ± 6.3 pl, which corresponds to a sphere with a diameter of 69.5 ± 8.4 μm. The droplets shrunk during the course of its flow through the continuous phase (Figs. 2(b)–2(f)) because of the dissolution of the water molecules from the droplets into the continuous phase. The droplet diameter at the second confluence point was 10.0 ± 0.7 μm (volume of 0.54 ± 0.12 pl) with a corresponding retention time of ∼1500 ms. The droplet volume at this point was ∼0.30% of the initial volume with the estimated alginate concentration of ∼33%. This indicated that a considerable amount of water was still present within the shrunk droplets, probably because of the hygroscopic nature of the alginate polymer. It should be noted that the droplets dissolved completely and therefore, disappeared when distilled water was used as the dispersed phase. In contrast, the volume of the droplets did not significantly change when water-saturated methyl acetate was used as the continuous phase. In this experiment, PDMS microchannel swelled with methyl acetate; the width of the microchannel increased from ∼200 μm to ∼210 μm by the introduction of methyl acetate, but it did not substantially affect the droplet generation process. Microfluidic devices made of other types of materials (glass, silicon, and solvent-tolerant polymers) could be also employed, if they have proper surface characteristics.

Previous studies have reported on the microfluidics-based formation of non-equilibrium droplets and their applications. Non-equilibrium W/O droplets have been prepared using dimethyl carbonate,[30,32,37] in which water has a solubility of 3%, and silicone oils, which are only slightly miscible with water.[35] Ethyl acetate, which can dissolve water at 3%, has also been employed to prepare droplets.[38] However, to the best of our knowledge, methyl acetate has not been used for producing W/O droplets. Among the solvents mentioned above, water has the high solubility in

methyl acetate (8%), and thus, the use of methyl acetate would result in the rapid extraction of water molecules from the droplets.

B. Production of Ca-alginate hydrogel beads

Next, we synthesized single micrometer-sized alginate hydrogel beads. Alginate is a biocompatible polymer obtained from seaweed, which rapidly gels in the presence of multivalent cations such as Ca^{2+} and Ba^{2+}. Because of the mild gelation conditions required, alginate hydrogels have been used for a variety of applications, including biological immobilization for bio-production,[39] patterned cell culture,[40] tissue engineering,[41,42] and cell transplantation therapies.[43] In this study, we introduced an aqueous solution of the gelation agent (1M $CaCl_2$) into the microfluidic device (with a dissolution channel length of 70 mm) at the second confluence point, by which time the droplet shrinkage was almost complete. In the gelation channel, the gelation solution and methyl acetate flowed parallelly when the flow rates Q_1, Q_2, and Q_3 ($=Q'_3$) were 30, 0.6, and 15 μl/min, respectively (Fig. 2(e)). The interface formed between the gelation solution and methyl acetate was clearly maintained along the entire length of the gelation channel. As the Ca^{2+} ions would not diffuse into the continuous phase, it was likely that the shrunken droplets came into contact with the gelation solution in the gelation channel, resulting in the formation of hydrogel beads.

Figure 3(a) shows the beads obtained when the initial NaA concentration was varied as indicated. Spherical alginate hydrogel beads with a narrow size distribution were successfully obtained. The surface of the beads was relatively rough, which might have been caused by the rapid dissolution and gelation of the droplets. The diameters and coefficient of variation (CV) values of the beads were 6.0, 7.0, 9.2, and 10.4 μm, and 6.0%, 2.6%, 4.5%, and 3.0%, when the initial NaA concentrations were 0.025%, 0.05%, 0.1%, and 0.15%, respectively (Fig. 3(b)). Smaller beads were obtained at lower NaA concentrations. The relation between the initial NaA concentration and the volume ratios of the beads to the initial droplets is shown in Fig. 3(c). The volume ratios were proportional to the initial NaA concentrations, indicating that the concentrations of the alginate polymer within the obtained beads were consistently ~40% regardless of the initial precursor concentrations. Thus, we confirmed that the sizes of the beads were precisely controllable by adjusting the precursor concentration and the initial droplet size.

Next, the characteristics of the Ca-alginate hydrogel beads were examined. After drying the beads overnight at 37 °C, the shape of the beads deformed due to the loss of water but it recovered after re-swelling in distilled water (Fig. 4(a)). This result indicated that the obtained beads

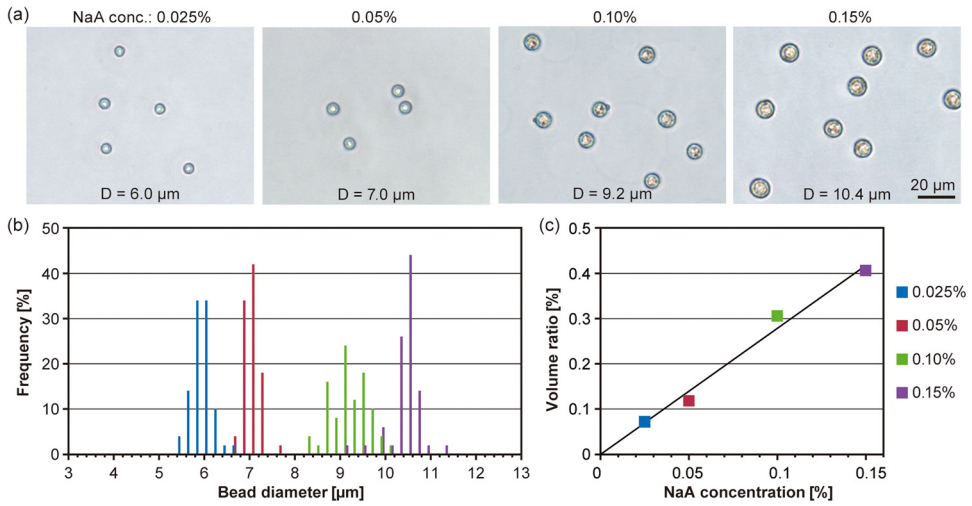

FIG. 3. Production of micrometer-sized Ca-alginate hydrogel beads. (a) Hydrogel beads produced from different precursor concentrations. (b) Size distributions of the obtained beads. (c) Relationship between the initial NaA concentration and the volume ratio of the beads to the initial droplets.

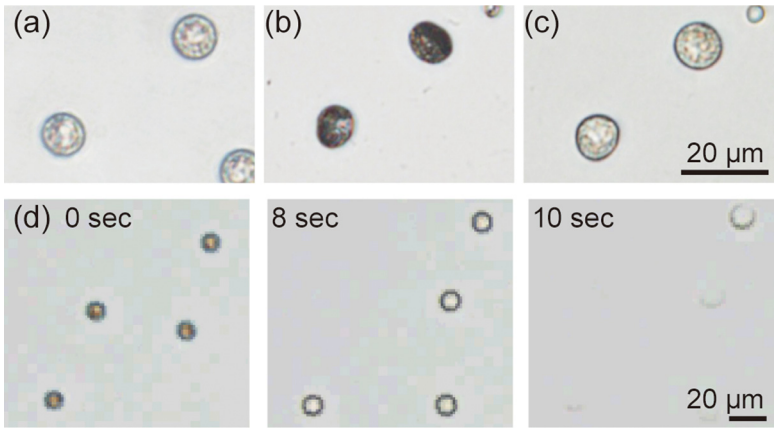

FIG. 4. Examination of the hydrogel nature of the obtained beads. (a)-(c) The obtained beads (a) before drying, (b) after drying overnight at 37 °C, and (c) re-swelled in distilled water. (d) Dissolution of the alginate beads by chelating Ca^{2+} ions using an aqueous solution of 0.1M trisodium citrate. Beads were dissolved within ∼10 s after dipping in the solution.

did contain water and were composed of hydrogel. In addition, the dissolution of the beads in an aqueous solution of 0.1M trisodium citrate solution, a chelating agent for Ca^{2+} (Fig. 4(b)), indicated that the beads were made of Ca-alginate.

In the previous studies, microfabricated nozzles, microchannels, or capillaries have been employed to produce monodisperse alginate hydrogel beads.[6,26,44] However, it was not easy to generate single micrometer-sized droplets of a viscous precursor solution, because of the high pressure required to introduce the solution into narrow channels or capillaries. Moreover, the physical stiffness of the hydrogel beads produced from a low concentration of the precursor solution (ex. 0.1% NaA) would not be sufficient for maintaining the bead morphology. In contrast, the presented technique is capable of concentrating the alginate polymer up to ∼400-fold, resulting in the formation of solid hydrogel beads. In addition, monodisperse single-micrometer-sized hydrogel beads were easily obtained owing to the use of a less viscous precursor solution at low concentrations and the dissolution process of the non-equilibrium droplets.

C. Control of bead morphology

The shape of the hydrogel beads plays an important role in determining its characteristics. In attempts to control the bead morphology, we first investigated the effect of the $CaCl_2$ concentration on the formation of non-spherical hydrogel beads, which would be closely associated with the gelation speed of alginate. The $CaCl_2$ concentration in the gelation solution was changed from 10 mM to 5M. The flow-rates Q_1, Q_2, and Q_3 were 30, 0.6, and 15 μl/min, respectively. When the $CaCl_2$ concentration was 5M, hydrogel beads with a size of ∼9.4 μm were obtained (Fig. 5(a)), which was similar to the beads obtained using 1M $CaCl_2$, as shown in Fig. 3. When the $CaCl_2$ concentration was decreased to 100 mM, the beads became slightly larger (∼10.7 μm) although their shape remained spherical (Fig. 5(b)). In contrast, teardrop-like

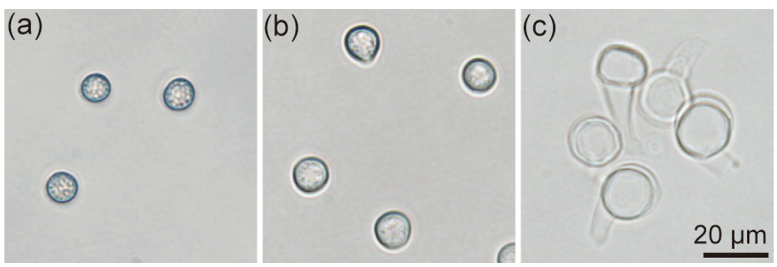

FIG. 5. Ca-alginate hydrogel beads prepared using gelation solutions with different $CaCl_2$ concentrations. $CaCl_2$ concentrations were (a) 5M, (b) 100 mM, and (c) 10 mM, respectively.

hydrogel beads were generated when the $CaCl_2$ concentration was 10 mM (Fig. 5(c)). This unique shape would be caused by the low gelation speed of alginate at low $CaCl_2$ concentrations; when the concentrated droplets migrated into the gelation solution from the continuous phase, the droplets swelled before gelation was complete, and the droplet shape was deformed because of the flow-induced shear stress, forming the tail structure.

Next, we investigated the effect of the degree of water dissolution (i.e., the degree of droplet shrinkage) on the bead morphology. Microfluidic devices with a shorter dissolution channel (22 mm) were used for this experiment. The behavior of the droplets and the obtained hydrogel beads are shown in Fig. 6. The flow rates Q_1, Q_2, and Q_3 were 30, 0.6, and 15 μl/min, respectively. Under these flow rates, the retention time of the droplets in the dissolution channel was ~500 ms. The droplet diameter at the second confluence point was ~38.8 μm and its volume was ~5.9% of the volume of the initial droplets whose average diameter was ~100 μm. We clearly observed that the shrunken droplets came into contact with the interface formed between the continuous phase and the gelation solution at several hundred micrometers downstream from the second confluence point. The obtained hydrogel beads exhibited unique mushroom-like morphology with an average width of 29.4 μm (Fig. 6(d)). The hydrogel matrices within these beads were less concentrated compared to those shown in Fig. 3(a). The formation of this non-spherical morphology would be a result of the non-uniform gelation process; a hemisphere of a droplet was initially deformed when the droplet was in contact with the interface and gelled. This was followed by the gelation of the other part of the droplet, which was away from the interface (Fig. 6(e)). Hydrogel beads with similar shapes have been reported previously, formed by droplet deformation either at the liquid/liquid interface[45,46] or in microchannels.[47,48] Together with these previous reports, the present study demonstrated the possibility for controlling the droplet shape by utilizing the interfaces in multiphase systems. It is worth noting that the flow

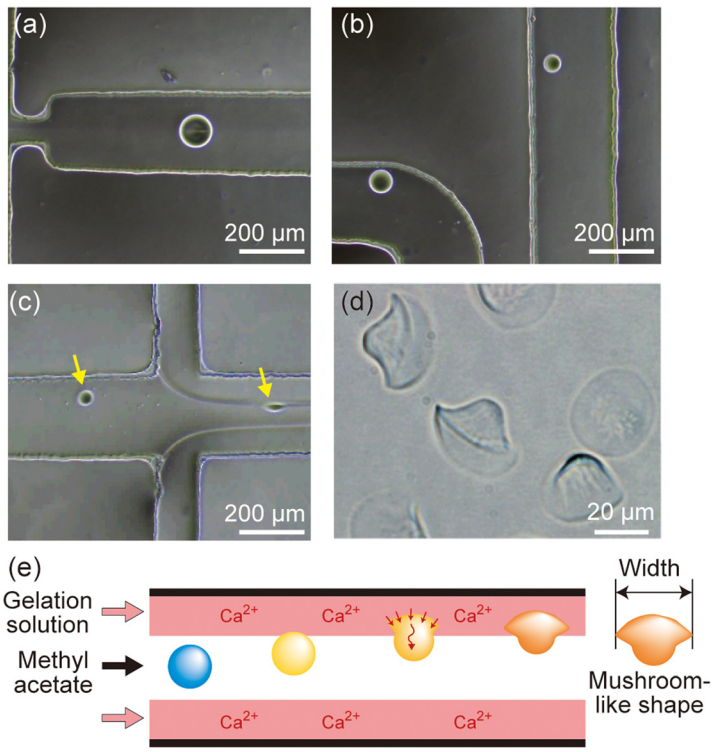

FIG. 6. Preparation of non-spherical hydrogel beads by controlling the degree of droplet shrinkage. A microfluidic device with a shorter dissolution channel (22 mm) was used. (a)-(c) Droplets at the first confluence point (a), in the dissolution channel (b), and at the second confluence point (c). In (c), arrows indicate the droplets. (d) Micrograph of the obtained mushroom-shaped hydrogel beads. (e) Schematic showing the mechanism of formation of the non-spherical hydrogel beads.

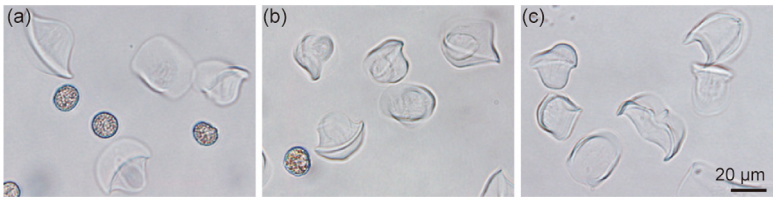

FIG. 7. Effect of the flow rate of the gelation solution on the ratio of the non-spherical Ca-alginate hydrogel beads. The flow rates of the gelation solution Q_3 ($=Q_3'$) were (a) 5, (b) 15, and (c) 60 μl/min, respectively.

rate of the gelation solution plays a critical role on the production efficiency of these mushroom-shaped beads, as it determines the flow width of the gelation solution in the gelation channel and thus the probability with which the shrunken droplets come into contact with the interface. When the flow rate of the gelation solutions (Q_3) was increased from 5 to 60 μl/min, the ratio of the non-spherical beads increased as shown in Figure 7.

D. Production of chitosan hydrogel beads

Next, we tried to extend the scope of the presented scheme to the production of other types of beads such as hydrogel beads made of chitosan. Chitosan is a polysaccharide derived from chitin and is widely used in medicine as carriers for DDS and tissue-engineering scaffolds because of its useful characteristics such as biocompatibility, biodegradability, and cell-adhesion.[49,50] To produce chitosan beads with sizes of several hundred nanometers, simple precipitation processes are often

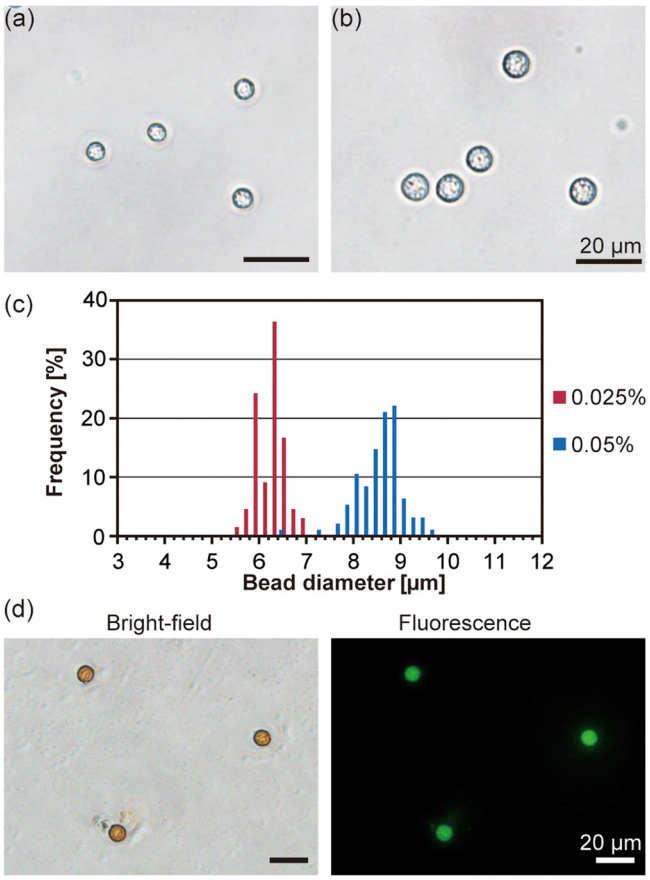

FIG. 8. Preparation of chitosan hydrogel beads. (a) and (b) Micrographs and (c) the size distributions of the hydrogel beads prepared from (a) 0.025% and (b) 0.05% chitosan solutions. (d) Bright-field and fluorescence images of the chitosan hydrogel beads prepared from 0.05% chitosan solution and conjugated with NHS-fluorescein.

employed.[51] Spray drier or vibration nozzle techniques have been reported for the production of chitosan hydrogel beads with sizes ranging from several micrometers to several millimeters.[52–54] Microfluidic devices have also been used to produce chitosan microbeads;[55,56] however, there are not so many reports on the production of chitosan beads with single micrometer diameters.[57] In this study, methyl acetate, a precursor solution (0.025% or 0.05% chitosan in 0.1M acetic acid aq.), and a gelation solution (1 mM NaOH aq.) were introduced into the microchannel under the same flow-rate conditions used for producing alginate hydrogel beads shown in Fig. 3.

In this case too, the droplets of the precursor solution were successfully formed in the continuous phase (methyl acetate) and then shrunken during the course of its flow through the microchannel. The obtained hydrogel beads and their size distributions are shown in Fig. 8. The average diameters of the hydrogel beads were 6.2 and 8.6 μm with CV values of 4.6% and 5.6%, at chitosan concentrations of 0.025% and 0.05%, respectively. The volume of the hydrogel beads was ~0.35% of the initial volume of the generated droplets for both concentrations, demonstrating that the bead sizes could be precisely controlled by changing the chitosan concentration. This result showed that the process presented in this study could be applied to the production of different types of hydrogel beads with single micrometer sizes. In addition, we were able to conjugate the amine group of the chitosan beads with NHS-fluorescein as shown in Fig. 8(d). This result suggests that the amine group of chitosan can be used for the further functionalization of the chitosan beads. Although various methods for preparing chitosan hydrogel beads have been proposed, the presented system is advantageous since it enables the preparation of monodisperse, single micrometer-size, and condensed chitosan hydrogel beads with a simple experimental setup.

E. Encapsulation of concentrated DNA in alginate hydrogel beads

To demonstrate the use of the prepared hydrogel beads for bio-encapsulation, we produced Ca-alginate hydrogel beads containing DNA molecules. NaA solutions containing λDNA

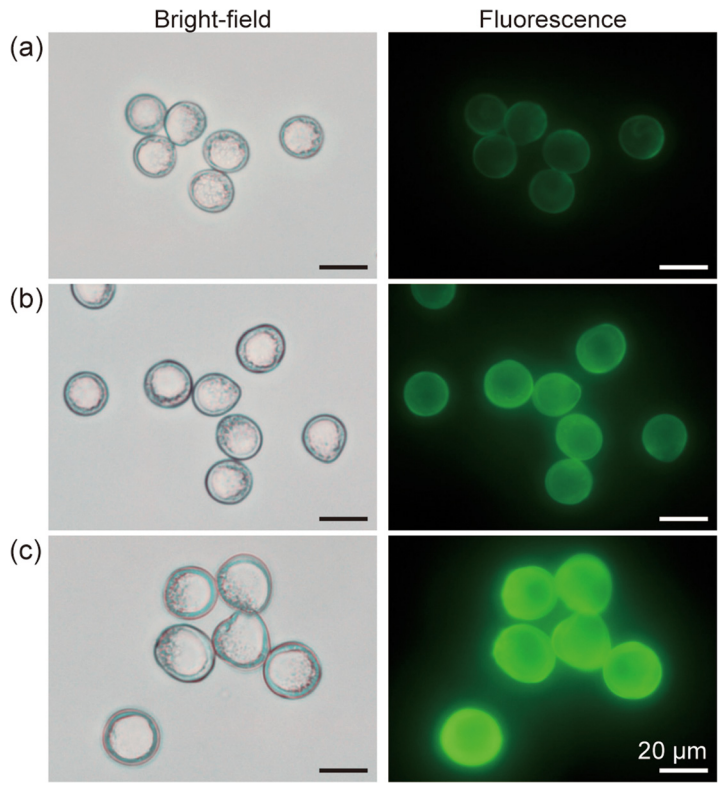

FIG. 9. Ca-alginate hydrogel beads incorporating λDNA. (a)-(c) Hydrogel beads made from 0.1% NaA solution containing (a) 50, (b) 100, and (c) 200 ng/μl of λDNA, respectively. DNA was stained with SYBR Green I.

molecules at different concentrations (50, 100, and 200 ng/μl) were used as the precursor. The flow rates Q_1, Q_2, and Q_3 were 30, 0.6, and 15 μl/min, respectively. The prepared hydrogel beads with encapsulated DNA molecules are shown in Figs. 9(a)–9(c). Hydrogel beads with an average size of 18–20 μm were obtained. The higher DNA concentration resulted in the slightly larger hydrogel beads formed, which would have been caused by the higher viscosity of the precursor solution and the larger size of the generated droplets. Because of the permeability of the hydrogel, the DNA molecules were rapidly stained with a green fluorescent dye, SYBR Green I, by dipping the beads in the dye solution. The fluorescence intensities of the beads were higher when the initial DNA concentration was higher. Owing to the large size of λDNA ($\sim$48 kbp), DNA molecules were stably encapsulated in the hydrogel matrices for at least a week. In this case, the volume ratio of the beads was $\sim$0.4% of the initial volume of the droplets. Assuming that the DNA molecules were perfectly encapsulated into the hydrogel matrices, the DNA concentrations were significantly increased ($\sim$250-fold). This result indicated that this process was capable of effectively enriching water-soluble macromolecules in the small hydrogel particles. Although we did not demonstrate the encapsulation of small molecules within the beads, such molecules would be gradually released from the hydrogel matrix depending on the molecule size and the sieve size of the hydrogel, because of the permeability of the alginate matrices.[58] Monodisperse hydrogel beads with encapsulated DNA molecules were recently applied in biochemical studies such as single molecule analysis.[59] We expect that the process presented in this paper for enriching biomolecules within cell-sized hydrogel beads would prove useful in biochemical research and clinical diagnosis, as well as the drug-releasing carriers.

IV. CONCLUSIONS

A process for producing single micrometer-sized, monodisperse hydrogel beads was demonstrated, by utilizing the non-equilibrium aqueous droplets formed in a polar solvent. Ca-alginate and chitosan hydrogel bead with precisely controlled sizes were produced, showing the applicability of the presented process to various types of hydrogel materials. In addition, by controlling the concentration of the gelation agent and the degree of water dissolution, hydrogel beads having non-spherical morphologies were generated. Moreover, encapsulation and concentration of DNA molecules within the hydrogel matrices were successfully demonstrated. The presented micrometer-sized hydrogel beads would be useful as innovative materials for various chemical/biochemical applications such as the cell cultivation scaffolds, carriers for DDS, sieving matrices for bio-separation, and analytical tools for biomacromolecules.

ACKNOWLEDGMENTS

This research was supported in part by Grants-in-aid (Nos. 23106007 and 25750171) and by Special Coordination Funds for Promoting Science and Technology from the Ministry of Education, Culture, Sports, Science, and Technology, Japan. We thank KIMICA Corporation, Japan, for kindly providing the alginate polymer.

[1]A. C. Jen, M. C. Wake, and A. G. Mikos, Biotechnol. Bioeng. **50**, 357 (1996).
[2]A. S. Hoffman, Adv. Drug Delivery Rev. **54**, 3 (2002).
[3]A. Y. Rubina, A. Kolchinsky, A. A. Makarov, and A. S. Zasedatelev, Proteomics **8**, 817 (2008).
[4]V.-T. Tran, J.-P. Benoît, and M.-C. Venier-Julienne, Int. J. Pharm. **407**, 1 (2011).
[5]S. Sugiura, T. Oda, Y. Izumida, Y. Aoyagi, M. Satake, A. Ochiai, N. Ohkohchi, and M. Nakajima, Biomaterials **26**, 3327 (2005).
[6]S. Sugiura, T. Oda, Y. Aoyagi, R. Matsuo, T. Enomoto, K. Matsumoto, T. Nakamura, M. Satake, A. Ochiai, N. Ohkohchi, and M. Nakajima, Biomed. Microdevices **9**, 91 (2007).
[7]Y. Morimoto, W.-H. Tan, and S. Takeuchi, Biomed. Microdevices **11**, 369 (2009).
[8]J. Dohnal and F. Štěpánek, Powder Technol. **200**, 254 (2010).
[9]H. Zhang, E. Tumarkin, R. M. A. Sullan, G. C. Walker, and E. Kumacheva, Macromol. Rapid Commun. **28**, 527 (2007).
[10]C. Kim, J. H. Bang, Y. E. Kim, J. H. Lee, and J. Y. Kang, Sens. Actuators, B **166**, 859 (2012).
[11]M. Marquis, D. Renard, and B. Cathala, Biomacromolecules **13**, 1197 (2012).
[12]L. Desbois, A. Padirac, S. Kaneda, A. J. Genot, Y. Rondelez, D. Hober, D. Collard, and T. Fujii, Biomicrofluidics **6**, 044101 (2012).

[13]B. G. Chung, K.-H. Lee, A. Khademhosseini, and S.-H. Lee, Lab Chip **12**, 45 (2012).
[14]M. Lian, C. P. Collier, M. J. Doktycz, and S. T. Retterer, Biomicrofluidics **6**, 044108 (2012).
[15]C. Young, K. Rozario, C. Serra, L. Poole-Warren, and P. Martens, Biomicrofluidics **7**, 044109 (2013).
[16]P. Panda, S. Ali, E. Lo, B. G. Chung, T. A. Hatton, A. Khademhosseini, and P. S. Doyle, Lab Chip **8**, 1056 (2008).
[17]D. Choi, E. Jang, J. Park, and W.-G. Koh, Microfluid. Nanofluid. **5**, 703 (2008).
[18]C.-H. Yeh and Y.-C. Lin, Microfluid. Nanofluid. **6**, 277 (2009).
[19]M. E. Helgeson, S. C. Chapin, and P. S. Doyle, Curr. Opin. Colloid Interface Sci. **16**, 106 (2011).
[20]S. K. Suh, S. C. Chapin, T. A. Hatton, and P. S. Doyle, Microfluid. Nanofluid. **13**, 665 (2012).
[21]M. S. Hahn, J. S. Miller, and J. L. West, Adv. Mater. **18**, 2679 (2006).
[22]J. Yeh, Y. Ling, J. M. Karp, J. Gantz, A. Chandawarkar, G. Eng, J. Blumling III, R. Langer, and A. Khademhosseini, Biomaterials **27**, 5391 (2006).
[23]C. Kantak, Q. Zhu, S. Beyer, T. Bansal, and D. Trau, Biomicrofluidics **6**, 022006 (2012).
[24]A. Miyama, M. Yamada, S. Sugaya, and M. Seki, RSC Adv. **3**, 12299 (2013).
[25]K.-S. Huang, M.-K. Liu, C.-H. Wu, Y.-T. Yen, and Y.-C. Lin, J. Micromech. Microeng. **17**, 1428 (2007).
[26]A. M. Chuah, T. Kuroiwa, I. Kobayashi, X. Zhang, and M. Nakajima, Colloids Surf., A **351**, 9 (2009).
[27]K. Maeda, H. Onoe, M. Takinoue, and S. Takeuchi, Adv. Mater. **24**, 1340 (2012).
[28]B. Wang, H. C. Shum, and D. A. Weitz, ChemPhysChem **10**, 641 (2009).
[29]C. Berkland, K. Kim, and D. W. Pack, J. Controlled Release **73**, 59 (2001).
[30]A. Fang, C. Gaillard, and J.-P. Douliez, Chem. Mater. **23**, 4660 (2011).
[31]A. Fang, C. Gosse, C. Gaillard, X. Zhao, and J. Davy, Lab Chip **12**, 4960 (2012).
[32]E. Rondeau and J. J. Cooper-White, Langmuir **24**, 6937 (2008).
[33]G.-R. Yi, T. Thorsen, V. N. Manoharan, M. J. Hwang, S.-J. Jeon, D. J. Pine, S. R. Quake, and S.-M. Yang, Adv. Mater. **15**, 1300 (2003).
[34]V. N. Manoharan, M. T. Elsesser, and D. J. Pine, Science **301**, 483 (2003).
[35]A. Q. Shen, D. Wang, and P. T. Spicer, Langmuir **23**, 12821 (2007).
[36]D. C. Duffy, J. C. McDonald, O. J. A. Schueller, and G. M. Whitesides, Anal. Chem. **70**, 4974 (1998).
[37]L. H. Hung, S. Y. Teh, J. Jester, and A. P. Lee, Lab Chip **10**, 1820 (2010).
[38]L. Liu, J. P. Yang, X. J. Ju, R. Xie, L. Yang, B. Liang, and L. Y. Chu, J. Colloid Interface Sci. **336**, 100 (2009).
[39]K. Koyama and M. Seki, J. Biosci. Bioeng. **97**, 111 (2004).
[40]S. Sugaya, S. Kakegawa, S. Fukushima, M. Yamada, and M. Seki, Langmuir **28**, 14073 (2012).
[41]M. Yamada, S. Sugaya, Y. Naganuma, and M. Seki, Soft Matter **8**, 3122 (2012).
[42]M. Yamada, R. Utoh, K. Ohashi, K. Tatsumi, M. Yamato, T. Okano, and M. Seki, Biomaterials **33**, 8304 (2012).
[43]J. Mei, A. Sgroi, G. Mai, R. Baertschiger, C. Gonelle-Gispert, V. Serre-Beinier, P. Morel, and L. H. Buhler, Cell Transplant. **18**, 101 (2009).
[44]W. H. Tan and S. Takeuchi, Adv. Mater. **19**, 2696 (2007).
[45]L. Capretto, S. Mazzitelli, C. Balestra, A. Tosi, and C. Nastruzzi, Lab Chip **8**, 617 (2008).
[46]Y. Hu, Q. Wang, J. Wang, J. Zhu, H. Wang, and Y. Yang, Biomicrofluidics **6**, 026502 (2012).
[47]K. Liu, H. J. Ding, J. Liu, Y. Chen, and X. Z. Zhao, Langmuir **22**, 9453 (2006).
[48]K. Liu, Y. Deng, N. Zhang, S. Li, H. Ding, F. Guo, W. Liu, S. Guo, and X.-Z. Zhao, Microfluid. Nanofluid. **13**, 761 (2012).
[49]A. Di Martino, M. Sittinger, and M. V. Risbud, Biomaterials **26**, 5983 (2005).
[50]I. Aranaz, M. Mengibar, R. Harris, I. Panos, B. Miralles, N. Acosta, G. Galed, and A. Heras, Curr. Chem. Biol. **3**, 203 (2009).
[51]H. Q. Mao, K. Roy, V. L. Troung-Le, K. A. Janes, K. Y. Lin, Y. Wang, J. T. August, and K. W. Leong, J. Controlled Release **70**, 399 (2001).
[52]W. L. Yan and R. Bai, Water Res. **39**, 688 (2005).
[53]S. Park, S. Hwang, and J. Lee, Chem. Eng. J. **169**, 348 (2011).
[54]Y. Lin, L. Zhang, W. Yao, H. Qian, D. Ding, W. Wu, and X. Jiang, ACS Appl. Mater. Interface **3**, 995 (2011).
[55]C.-H. Yang, K.-S. Huang, and J.-Y. Chang, Biomed. Microdevices **9**, 253 (2007).
[56]C.-H. Yang, Y.-S. Lin, K.-S. Huang, Y.-C. Huang, E.-C. Wang, J.-Y. Jhong, and C.-Y. Kuo, Lab Chip **9**, 145 (2009).
[57]H. Zhao, J.-H. Xu, P.-F. Dong, and G.-S. Luo, Chem. Eng. J. **215–216**, 784 (2013).
[58]R. H. Li, D. H. Altreuter, and F. T. Gentile, Biotechnol. Bioeng. **50**, 365 (1996).
[59]H. Zhang, G. Jenkins, Y. Zou, Z. Zhu, and C. J. Yang, Anal. Chem. **84**, 3599 (2012).